Confinement Effect of Woven Roving Glass Fabric on Concrete Specimen

Smitha Gopinath[1,2]**, A. Ramachandra Murthy**[1]**, Bhaskar Srivastava**[1]
V. Ramesh kumar[1] **and Nagesh R. Iyer**[1]

Abstract: The present study investigates the behavior of concrete specimens confined with woven roving glass fabrics under uniaxial compression. The fabric made up of 360G.S.M. woven roved E-glass is embedded in a polyester resin before application. Experimental investigations have been carried out on confined and unconfined concrete specimens of size 150 mm (diameter) X 300 mm (height) under a displacement controlled loading. The effect of number of layers on confinement has also been investigated. Load versus deflection plots have been obtained for all the specimens. Numerical studies have been performed on the confinement effect of the wrapped concrete specimens. A non-linear finite element analysis has been conducted by developing numerical models in a general purpose finite element commercial software ABAQUS. The results obtained by numerical study have been compared and validated with the corresponding experimental results. Parametric studies have been conducted to study the effect of confinement on the response of the specimens. The parameters affecting the confinement were found to be the grade of concrete and number of layers of the fabric. Further, mesh sensitivity analysis has also been carried out to find out the mesh dependency of the confined specimens and results have been presented.

Keywords: Woven roving, Confinement, Strengthening, Uniaxial Compression, Finite element, Nonlinear analysis, Mesh sensitivity.

1 Introduction

Structural strengthening is a major challenge in front of civil engineers as it is not only a continuous task but also an inevitable one as eventually every structure at the end of its service life needs strengthening. It is also economically and ecologically more desirable to rehabilitate a structure than to create an entirely new one replac-

---

[1] CSIR - Structural Engineering Research Centre, Taramani, Chennai-600113, India
[2] Corresponding Author: smithag@serc.res.in, smithagopinath13@yahoo.com

ing it. Strengthening a structure by FRP confinement has gained recent popularity. After the earlier attempts by [Kurt (1978)] and [Fardis and Khalili (1981, 1982)] a remarkable amount of experiments have been performed to investigate the behavior of concrete columns confined with FRP spirals [Ahmad et al. (1991); Nanni and Bradford (1995)] wraps [Harmon and Slattery (1992); Picher et al. (1996); Watanabe et al. (1997); Miyauchi et al. (1997); Toutanji (1999); Matthys et al. (1999); Rochette and Labossie're (2000); Micelli et al. (2001); Rousakis (2001)] and tubes [Saafi et al. (1999); Fam and Rizkalla (2000); Ye et al. (1998)] conducted experimental investigations on a concrete column of 300 mm high and 150 mm diameter for confinement effect of E-glass woven roving (WR), combined with chopped strand mat (CSM) and glass fiber tape (GFT). It was concluded that use of E-glass fibers and the vinyl-ester resin to reinforce concrete columns externally is effective, with a low raw materials cost. [Xiao and Wu (2000); Lam and Teng (2004); Gu and Zu (2006)] conducted experimental investigations on concrete cylinders wrapped with FRP composites. The strength of FRP confined concrete was increased compared to the unconfined concrete, between 1% and 420% depending on the type and amount of FRP composite.

[Shahwy et al. (2000); Laura De Lorenzis et.al (2003); Wu et al. (2007)] conducted a detailed study about different numerical models for confinement. [Sangeetha (2007)] performed numerical analysis using Finite Element Method (FEM) against published experimental data to investigate the behavior of concrete columns, confined by FRP sheets under uniaxial compression. It was concluded that multiple placements of FRP plies improve the overall performance for square, rectangular and circular sections.

[Benzaid et al. (2008)] analyzed experimental results in terms of load-carrying capacity and strains obtained from tests on square prismatic concrete column, strengthened with external glass fiber composite. It was concluded that the external confinement with reinforced polymer composites can significantly increase the strength of the specimen under axial loading. [Saravanan et al. (2010)] carried out an experimental study on GFRP confined high strength concrete columns with a view to evaluate its performance under uniaxial compression in terms of load and deformation capacity. They used high strength concrete columns strengthened with different configurations and stiffness of GFRP wraps and tested them under axial compression until failure. Their response was evaluated at different load levels. The test results clearly indicated that, GFRP wrapped high strength concrete columns exhibits enhanced performance.

From the reported literature on the confinement effect of glass fabric, it can be concluded that use of E-glass fabric in epoxy resin is an effective strengthening system. Regarding the numerical investigations reported earlier, most of the models

over estimated the strength of the confined sections and confirms the necessity of developing more accurate and reliable models in this field.

The present work aims to enhance the understanding of confined concrete members under compressive load and evaluate the performance of E-glass woven roving fabrics in strengthening of concrete members. Glass fabric layers were wrapped on concrete cylinders and compressive strength of these cylinders were tested. Comparisons were made between single layer confining system, double layer confining system and the unwrapped concrete cylinder. Apart from the experimental investigations, analytical investigations have also been incorporated in this study. A non linear fabric confinement model has been developed using a commercially available finite element software ABAQUS. The model has been analyzed by varying the number of layers in the confinement model and a comparison has been performed. The results of the Finite Element study are in fair agreement with the experimental results. Mesh sensitivity analysis has also been carried out to find out the mesh dependency of the confined specimens. Further, parametric studies have also been conducted to study of effect of confinement on the response of the specimens by varying grade of concrete and number of layers of the fabric.

2 Experimental Details

The experimental program was executed to evaluate effectiveness of confinement of woven roving on concrete cylinders by by testing confined and unconfined specimens.

2.1 Specimen fabrication

The concrete cylinder of diameter 150mm and height 300mm were used for confined and unconfined concrete specimens. The mix for concrete cylinder was designed according to BIS standards for M30 grade concrete. The rich mixture of concrete is made by 1 volume of cement to 1.27 volume of sand and 2.78 of coarse aggregate. The water cement ratio adopted was 0.45.

2.2 Organic Resin as Binding material

The resin used is thixotropic accelerated and has a viscocity that ensures thorough glass fibre impregnation. It is easy to mix and can be applied by brush. The physical and mechanical properties of the resin is given in Table 1.

2.3 Woven roving

The type of glass fabric used in the present investigation is bi-directional woven roving glass fabric with $0^o/90^o$ orientation (Fig. 1). Typical properties of the same

Table 1: Physical and mechanical properties of resin

Polymer	Tensile strength (MPa)	Elongation	Density (g/cm^3)	Heat Distorsion Temperature
polylite	72	4.5%	1.2	85°C

are as follows (Table 2 & Table 3):

Table 2: Commercial Properties of the fabric

Fabric name	Density (No. of Ends/cm)		Area Weight g/m^2	Weave	Moisture Content (%)	Combustible Content (%)
	Warp	Weft	ISO 3374		ISO 3344	ISO 1887
EWR360	3.20	1.80	354 ± 18	Plain	≤ 0.15	0.40 ∼ 0.80

Table 3: Mechanical Properties of the fabric

Typical Properties	E-Glass
Density (g/cm^3)	2.60
Young's Modulus (GPa)	73
Tensile Strength (GPa)	3.4
Tensile Elongation (%)	2.4

2.4   Experimental Details

The specimens were tested using MTS machine of 2500kN capacity. In each specimen, two LVDT's has been fixed and connected to data acquisition system to measure axial deformation. Before the testing, the specimens were checked dimensionally and a detailed visual inspection was made and all informations were carefully recorded. Also, sulphur capping has been done to ensure the uniform load transfer to the specimen. After setting both the LVDTs, slowly the loading frame was given displacements and the equivalent load and deflections were recorded simultaneously. The tests conducted were according to the American Society of Testing and Method (ASTM) standards for all the specimens. Test has been carried out under displacement controlled loading. Uniaxial Compressive testing on the different fabric confined specimens were performed. The details of tests are elaborated below.

Figure 1: Woven Roving E-Glass Fabric

2.4.1 *Unconfined Specimen*

The maximum strength for the control cylinder (unconfined) tested in displacement control mode was 38.4 MPa. Typical failure of control cylinder was observed to be cone and lateral shear. A control cylinder after testing can be seen in Figure. 2.1 for cone failure & Figure. 2.2 for lateral shear failure.

Compressive stress values for the cylinder was calculated based on the area of the concrete cylinder and the axial strain was calculated as the average change in the length over the original length of the cylinders. The stain corresponding to the peak stress value for the plain specimen was 0.0027 mm/mm. From the post peak behavior it can be easily noted that after the specimen fails no appreciable strength is left in the structure. Beyond a strain value of 0.004, a sharp decrease in strength is observed. Figure 3 represents the stress strain behavior of the plain specimen using the load and displacement data obtained during the test.

2.4.2 *Details of specimens confined with woven roving*

Six cylinders wrapped with woven roving were tested in displacement control mode in order to capture the post peak behavior of the specimen. The loading rate till
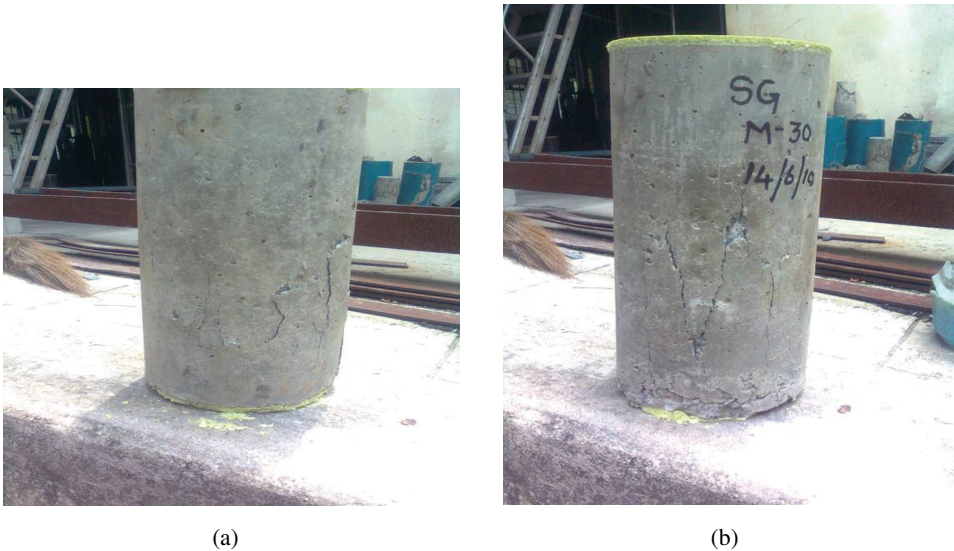
(a)   (b)

Figure 2: (a)Plain sample after test (Cone Failure); (b)Plain sample after test (Lateral Shear)
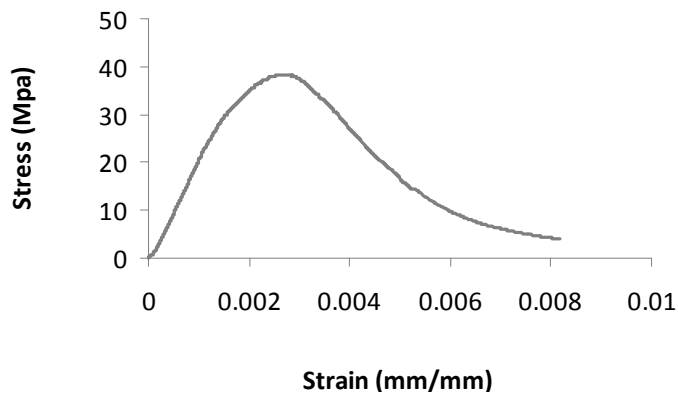

Figure 3: Stress vs. Strain Plot of the Plain Specimen

~0.0015 strain value was 0.2 mm / minute and after that the rate was 0.02 mm / minute. Specimens wrapped with single layer woven roving and double layer woven roving were also studied.

Specimen wrapped with 1Layer of WR

All the four single layered specimens (wr-1, wr-2, wr-3, wr-4) were tested in similar setup and the behavior of each specimen was individually recorded. The stress

strain curve of each specimen was obtained in the same way as for the plain member. The post peak behaviors for all wrapped cylinders were different than that of the control cylinder. Wrapped cylinders (WR) reached higher peak loads and accommodated larger displacements than the control cylinders. This is especially evident in Figure. 4, where stress vs. strain curves from both control and wrapped specimens are plotted by normalizing with respect to the plain specimen.

The energy absorbed by the samples play a very important role in enhancing its life under any kind of load, especially seismic loads. The greater the energy absorbed, the greater is the duration for which a specimen can sustain a given type of load. The area under any stress-strain curve gives an idea of the energy absorbed by the specimen during its loading. Hence, the area under the stress-strain curve of each sample was analyzed and compared with the plain sample to understand the effect of wrapping on the specimen under loading. The area under the stress-strain curve of the WR cylinder specimen was approximately 1.5 times larger than the area of the control cylinder (Table 4). Samples wr-2 and wr-4 had approximately 10% more area under the stress-strain curve than wr-1 and wr-3.
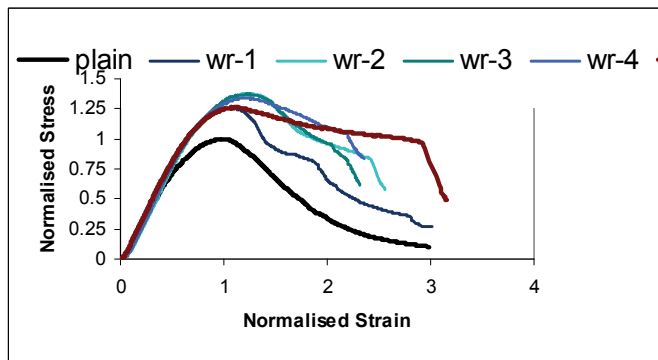

Figure 4: Normalized Stress Strain plot of all the specimens

Two Layer woven roving

The 2 Layer wrapped specimen (2lay WR) showed highly enhanced ductile property when compared to the previous samples. As evident in Figure 4, the 2LayerWR sample has the maximum area under the curve, approximately 2 times the area under the plain stress strain curve and 30% more than that under single layer WR curves (Table 4).

Owing to the increased energy absorption the failure in each of the wrapped sample was largely brittle with sudden rupture of the fabric, however minor change in modes of failure was observed in each case.

Table 4: Area under the curve for different specimens

Specimen	Plain	wr-1	wr-2	wr-3	wr-4	WR (avg)	2LayWR
Area Under Curve (wrt to plain)	1	1.45	1.61	1.49	1.57	1.53	2.04

2.4.3   Modes of Failure

For all the specimens wrapped with WR, the high energy absorption resulted in sudden failure due to sudden release of the absorbed energy. Minor changes in the failure modes were observed for different specimens with respect to control. The failure of each specimen is discussed here under.

wr-1

Tensile rupture of fabric occurred in this specimen. The fabric split along the length of the cylinder (Figure 5). The crack in the fabric initiated from the centre and propagated along the length. Around 45% more energy absorption was observed in this sample, this elicits the effect of the wrap. The post peak hardening was not appreciable; this could be possible because of debonding of the fabric from the concrete surface, as seen by the white patches visible on the surface due to which the wrap failed to provide stiffness to the material post failure. However, an increase in strength was observed; the sample failed at a peak stress of ∼ 48 MPa, i.e. 1.26 times the plain sample, the failure as already mentioned was sudden and this can also be noticed by a sudden almost vertical drop in the stress strain curve of the sample as shown in Figure 4. *wr-2*

The failure in this case also was sudden occurring at a strain of 0.0067(mm/mm) with sounds indicating the yielding of the fabric. The specimen failed at a peak stress of 52.88 MPa with corresponding strain of 0.00335. This sample showed the highest increase in strength compared to other single layer wrapped samples. The white patches indicative of debonding between the fabric and the concrete surface appeared first after a strain of 0.0045(mm/mm) as a result of which appreciable post peak strengthening is observed in the specimen stress strain curve as shown in Figure 6. Hence as expected this specimen absorbed the maximum amount of energy amongst all other single layer wrapped specimens. The area under the curve for this sample was 60% more than the plain sample. At the strain of 0.0067(mm/mm), a sudden drop in the curve can be seen from the Figure.4, this is the point where the specimen has completely collapsed and the stiffness has drastically reduced.

wr-3

The mode of failure was almost similar to that of the wr-1 sample, but the wr-3

Figure 5: wr-1 specimen

Figure 6: wr-2 specimen

sample absorbed greater amount of energy and had a peak stress value higher than wr-1. The peak stress value attained by the WR-3 sample was 52.7 MPa and the strain corresponding to this stress value was 0.00332, nearly as much as that of wr-2 at peak stress. The ductile behavior of this sample was also considerably enhanced. The energy absorbed by the sample was 0.49 times the plain sample and the end failure was due to the rupture of the fabric. The debonding between fabric and concrete was considerably less compared to other samples, as is visible from the Figure. 7; this could a possible explanation for the post peak hardening observed in Figure. 4. The specimen ultimately collapsed at a strain of 0.0058 mm/mm.

Figure 7: wr-3 specimen

wr-4

The behavior of this sample was a little improved over the other single layer wrapped samples in terms of the post peak hardening (Figure.4). The sample ultimately collapsed at a strain of 0.0061 mm/mm with progressive yielding of the fabric and could reach a maximum stress of 51.6 MPa at a strain of 0.00332. This sample showed a comparatively a stiffer post peak response which is desirable. The energy absorbed by this specimen is comparable to that of the WR-2 specimen even after collapsing at a lower strain value. The end failure was brittle with sudden collapse

Figure 8: wr-4 specimen

of the specimen(Figure 8).

The specimen also developed white patches due to the debonding phenomenon. Crack propagation was observed to start from the centre slowly progressing towards the top. All the above details have been summarized in Table 5.

Two Layer WR

The double layered WR wrapped sample showed some interesting observations. The overall strength achieved by the specimen was not high against the expected; the specimen could sustain a peak stress of only 48.59 MPa i.e. only a 27% increase over the plain specimen compared to an average 34% increase in the case of single layered samples. The possible explanation of this could be that in the very early stage the specimen started to exhibit white patches (Figure 9) indicative of the debonding between the two layers of the fabric wrap and hence the strength obtained for the sample was in the range of single layer WR samples (48-53 MPa) (Table 5). The energy absorbed was the largest in this case and was observed to be 200% more than the plain specimen. The specimen showed highly improved ductile properties and the post peak hardening was much better than any of the single layer samples. This could be because of the increased thickness of the wrap

(double layer). Although, only one specimen was wrapped with double layer glass fabric, the results obtained are fairly acceptable. Previously discussed modes of failure and other details as inferred from the test data are tabulated in Table 7.

Figure 9: 2 layer Wrapped specimen

3 Finite Element Analysis

Finite element analysis has been carried out on the cylinders wrapped with woven roving glass fabric using ABAQUS software. Three dimensional finite element models for the plain, single and double layer wrapped concrete cylindrical specimens were developed. Each concrete specimen of size 150mm in diameter and 300mm in height have been modeled using ABAQUS employing the C3D8R element. Concrete was assigned hexahedral mesh elements of size 20. Concrete has been considered as isotropic non linear elastic element. The glass fabric has been meshed using tetrahedral elements of size 15. This has been done to obtain a better contact of concrete and the glass fabric. C3D4 element type used to mesh the glass fabric. The thickness of a single layer of woven roving glass fabric has been taken as 1 mm. Fig. 10 shows the finite element model used for confined concrete cylinders.

Table 5: Performance under Uniaxial Compression of different samples

Specimen	Peak Stress (Relative)	Strain at Peak Stress (Relative)	Peak Stress (absolute)	Failure Type
Plain	1 (38.41MPa)	1 (0.0027)	38.41 MPa	Cone and Shear type failure
wr-1	1.26	1.07	48.37 MPa	Tensile rupture of woven roving fabric, 45% more energy absorption than plain sample
wr-2	1.38	1.24	52.88 MPa	Yielding of fabric after concrete failure
wr-3	1.37	1.23	52.73 MPa	Tensile rupture, enhanced ductile properties
wr-4	1.34	1.23	51.63 MPa	Enhanced ductile properties, yielding of fabric, failure at a strain of 0.0061
2LayWR	1.27	1.11	48.59 MPa	Debonding of WR layers and then rupture of fabric

The cylinder undergoes uniaxial compression and hence the bottom surface has to be fixed in all three directions of motion and the top surface is allowed to move in only one direction, as shown in Figure 11. A displacement of 1.5 cm has been given to the top surface (in lieu of an equal amount of load) which ABAQUS applies in several increments ensuring a converging solution at every increment.

Analysis is carried out by displacement controlled approach inorder to capture the nonlinear behaviour of woven roving confined concrete cylinders.

3.1 Material Modelling

Nonlinear behavior of concrete in compression and linear elastic behavior of glass fabric has been accounted for material modeling. An elastic and perfectly-plastic (or the classic metal plasticity model) material model has been chosen to define the concrete behavior. Table 6 lists the elastic properties of the concrete used in the
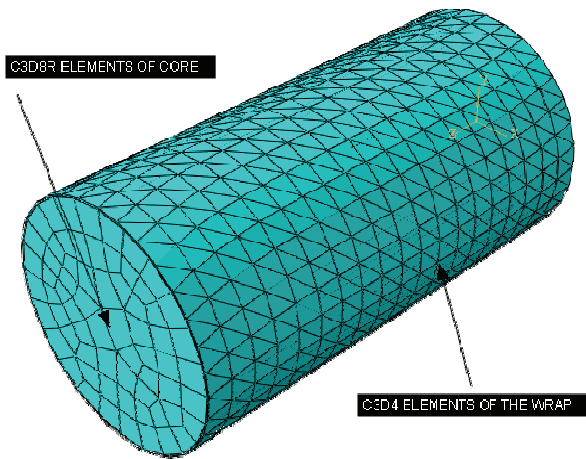
Figure 10: FE model of the single layer wrapped specimen

Figure 11: Specimen boundary conditions

analysis. The plastic properties i.e. the plastic strain and the yield stress data was obtained from the stress-strain graph of the unconfined M30 concrete column as shown in Figure 12

Where, E_c is the short term static modulus of elasticity in N/mm^2 and f_{ck} is the characteristic compressive strength of the concrete in N/mm^2 (in this case 30 N/mm^2).

Table 6: Properties of the concrete

Modulus of Elasticity (MPa)	Poisson's Ratio
27386	0.2

For material modeling of glass fabric, the material properties used are given in Table. 7 .Material model used in the studies is developed based on the elastic behavior of the fabric.

Table 7: Properties of the Glass Fabric

Modulus of elasticity (MPa)	73,000
Poisson's Ratio	0.15
Tensile strength (MPa)	3400
Ultimate elongation	2%

3.2 Interface modeling

Since two separate parts of concrete and woven roving confinement have been developed, in order to make them a single unit, a suitable interaction between them have been defined. A surface based tie constraint was defined in between the two parts in the present study. The interface between concrete specimens confined with the glass fabric has been modeled using surface to surface contact algorithm available in ABAQUS for the present study. The true surface-to-surface approach optimizes the stress accuracy for a given surface pairing. The choice of slave and master surfaces can have a significant effect on the accuracy of the solution. In the present study the concrete has been taken as master surface and woven roving fabric has been accounted for slave surface. To account for the relative motion of the two surfaces forming a contact pair in mechanical contact simulations, Finite sliding tracking approach is used. In the present study Finite sliding methods has been used. For finite-sliding contact the connectivity of the currently active contact constraints changes upon relative tangential motion of the contacting surfaces. For constraint enforcement the direct method has been accounted. The direct method is

the only method that can be used to enforce softened pressure-over closure relation-ships. A hard contact pressure-over closure relationship is used for surface-based contact.

3.3 Results and Discussions

The results obtained from analysis of each specimen are discussed with respect to corresponding experimental model and then a comparative study of the models is carried out. Plain cylinder from the finite element analysis was observed to have a failure load of 36.9 MPa and the stress v/s strain (plotted from load versus de-flection curve obtained from ABAQUS) is shown in Figure 12. It can be observed
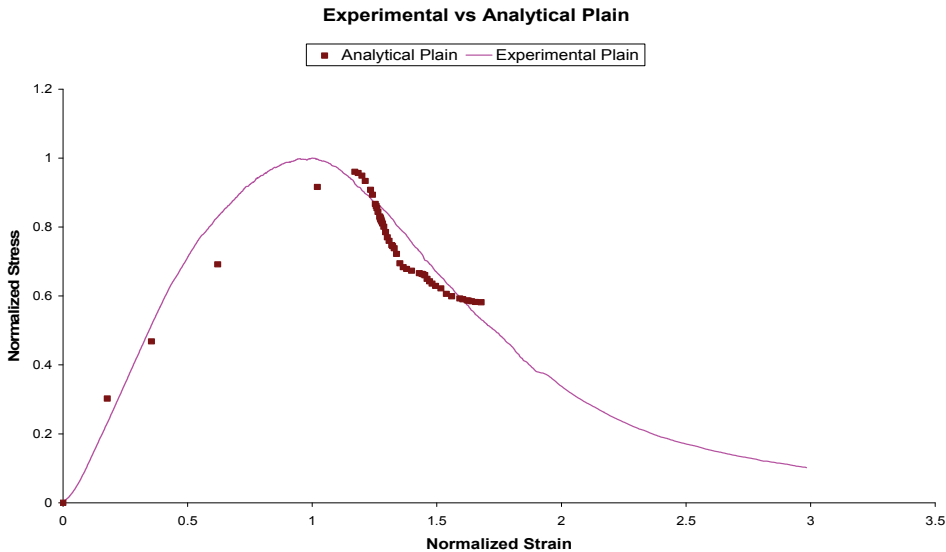
Figure 12: Experimental v/s Analytical Plain

from Figure 12 that, the behavior of the analytical model for plain concrete based on the elastic-perfectly plastic material model is in very good agreement with the experimental plain model. The peak strength is 95% of that of the experimentally observed value. Hence the predictions are very close and can be used safely.

The single layer glass fabric wrapped model predicts the behavior of the experi-mental studies successfully as can be seen in the Figure 13. The analytical model predicts the behavior correctly only till a specified strain value after which the con-crete core loses its stiffness completely but the fabric retains it stiffness and overall stiffness increases drastically.
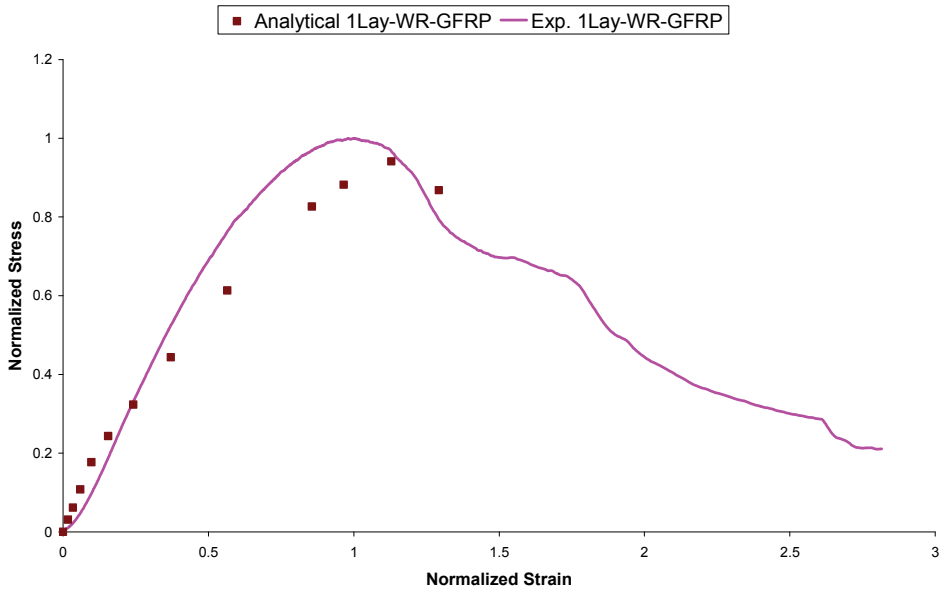
Figure 13: Analytical Single Layer Wrapped Model v/s Experimental Model

Peak strength obtained from analytical model is 45.5 MPa i.e. 90% of the experimental model at a strain of 0.0033 mm/mm. The results are observed to be close to the experimental values.

The analytical model for the double layer confinement could sustain a greater strength than the experimental model.

Two Layer WR, the experimental model underwent debonding of fabric at a very early stage and hence two layers of confinement could not play any role in strength enhancement. The double layered analytical model has the elastic and the pre-peak behavior similar to the double layer sample and fails to predict the highly ductile behavior of the double layer sample as observed in the experimental study (Figure 14). The maximum strength sustained by this model was 52.2 MPa. The maximum strain till which the model could successfully predict the behavior of the experimental model was 0.0037 mm/mm. The stress-strain graph comparing the analytical and the experimental models is shown in Figure 14. The figure shows the initial tangent modulus of the experimental and the analytical model to be nearly similar.

The Figure 15 shows the stress strain curve of each specimen with respect to plain analytical model. The peak stress and the corresponding strain value of the analyt-
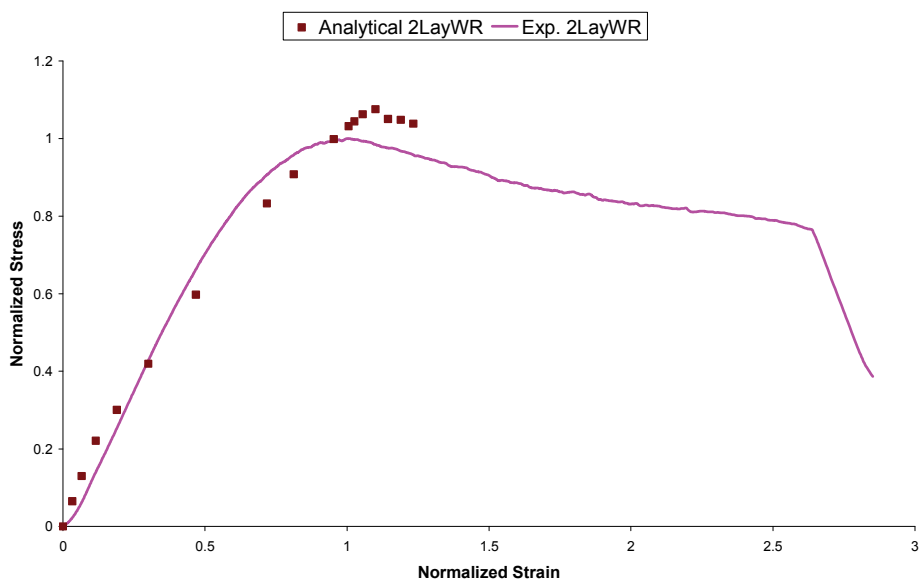
Figure 14: Analytical v/s Experimental double layer wrapped models

ical model are taken as unity. This helps to clearly assess the percentage increase in strength with each layer of confinement. Table 8 gives a comparison between ultimate strength of confined specimens over plain concrete specimen.

Table 8: Comparison of analytical models on strength

Specimens	Strength	Increase over plain
Analytical Plain	36.9 MPa	-
Single Layer Wrap of Glass Fabric	45.5 MPa	23%
Double Layer Wrap of Glass Fabric	52.2 MPa	41%

Figure 16 shows the stress contours for plain, 1layer wrapped and 2-layer wrapped specimens.

It is observed that the stress developed due to a displacement load of 1.5 cm is maximum in the central area of the single and double layer models and just at the beginning of the bulge in the plain model. With every layer of wrap the effect of confinement generally increases. The lateral strain developed is lowest in the case of double layered model as expected (Figure 17).

Table 9 lists the lateral strain developed in each of the model.
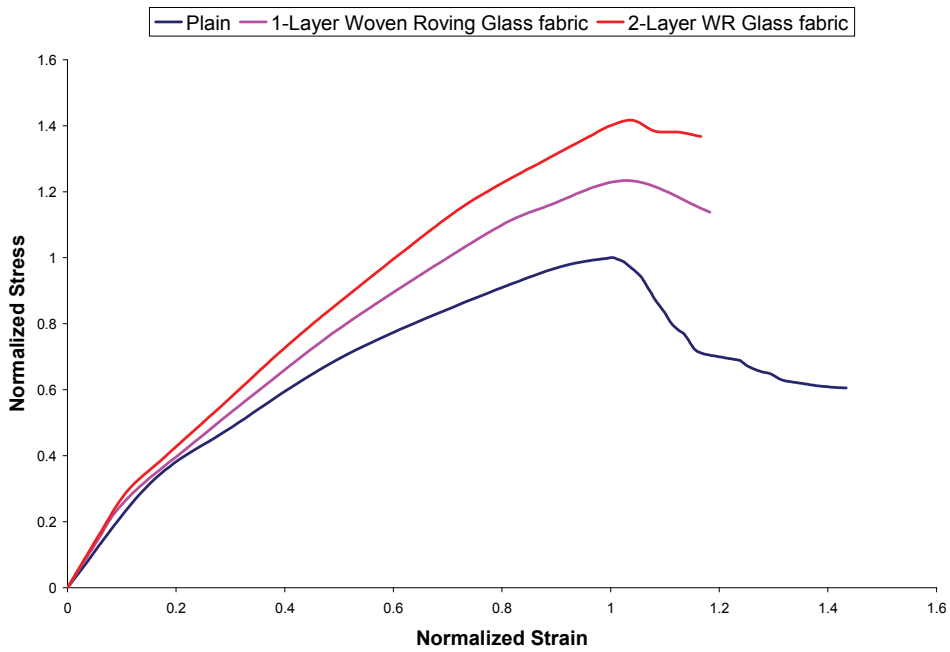
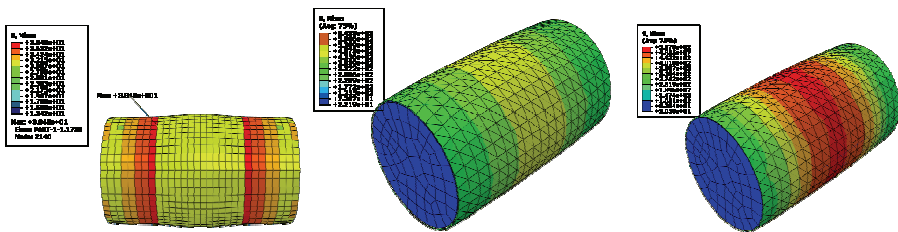Figure 15: Normalized stress v/s strain plot of analytical models

Figure 16: Stress contour of confined and unconfined models

Table 9: Lateral strain developed in each model

Specimens	Lateral Strain (in one direction)	Decrease over plain
Plain	0.26 mm	-
Single layer wrapped	0.21 mm	19%
Double layer wrapped	0.19 mm	27%

(a) Plain   (b) Single layered model   (b) Double Layered model
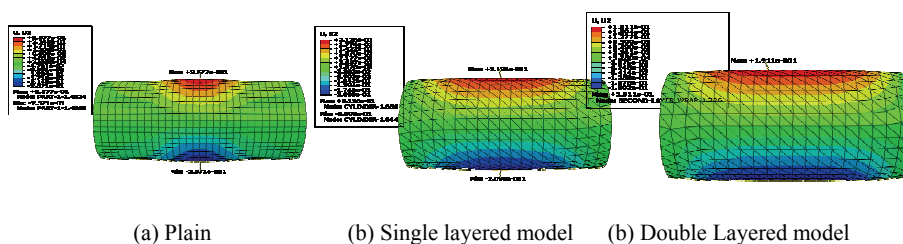
Figure 17: Lateral Strain contour of the analytical models

3.4   Mesh Sensitivity Analysis

Since meshing plays a very important role in a finite element analysis in many ways, it is important to choose the right mesh attributes in order to save computation time and also to achieve more accurate results. Based on this notion, mesh sensitivity analysis has been performed on the analytical models. The analysis is done on two mesh parameters namely, mesh element and mesh size.

3.4.1   Effect of mesh element on strength of the model

In the present investigation, the mesh element chosen for meshing the glass fabric was a 4 node tetrahedral element (C3D4) instead of a C3D8R element which was chosen to mesh the concrete cylinder. This was because a better contact between the concrete and the glass fabric was obtained in case of a tetrahedral element. A mesh sensitivity analysis was done to see the impact of: the type of mesh element on the contact algorithm and hence on the strength on the model. Figure 18 shows two models one with a hexahedral (HEX) mesh element for the glass fabric and the other with a tetrahedral (TET) mesh element while mesh element for the concrete core in both the cases is hexahedron element (C3D8R). The deformation in the HEX element case is not smooth and it shows that the contact is non uniform in the area with greater expansion. While for TET elements the deformation indicated a uniform bond between the fabric and the concrete core.

The overall strength of the model was also less in the case of HEX element meshing of the glass fabric as mentioned in Table 10. It should be noted that the effect of mesh element was studied only for single layer of confinement.

The effect of mesh element size on the strain energy of the model is studied and an optimum mesh size is obtained. The present sensitivity analysis is performed on a plain concrete model with HEX mesh elements and the sizes tested are 10, 15 and 20. The results are reported in the Table.11
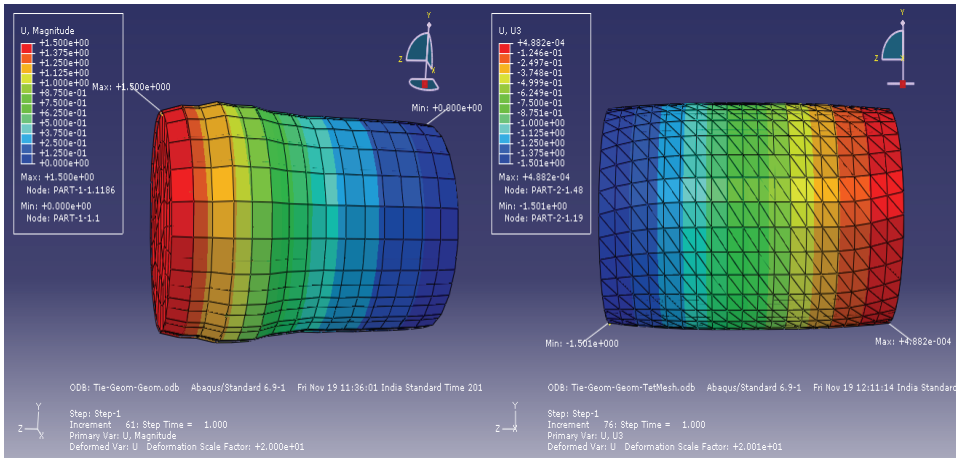
Figure 18: Deformation in case of HEX and TET elements

Table 10: Effect of mesh element on strength of the model

Mesh Element	Strength	Increase over HEX
HEX	41 MPa	-
TET	45.5 MPa	11%

Table 11: Effect of mesh size on the strain energy of the model

Mesh Size	Strain energy of the whole model
10	132.24 J
15	133.9 J
20	130.8 J

As is clear from the above results the strain energy for a mesh size of 20 is lowest and hence the model with a mesh size of 20 will be the most stable of the three. Therefore, the size of the mesh element was chosen to be 20.

4 Parametric Studies

Since the analytical models so far developed are in fair agreement with the experimental results obtained, implying that the model of confinement created by authors are acceptable. Now we intend to understand the effect of confinement of the same fabric in some other conditions. A basic parameter, the grade of concrete, is changed to study the confinement effect of our glass fabric on these grades of

concrete. The M40 and M50 concrete properties were obtained from the experimental results available in the literature and a finite element model for each grade was created and analyzed. The behavior of the same is as shown in Figure 19.
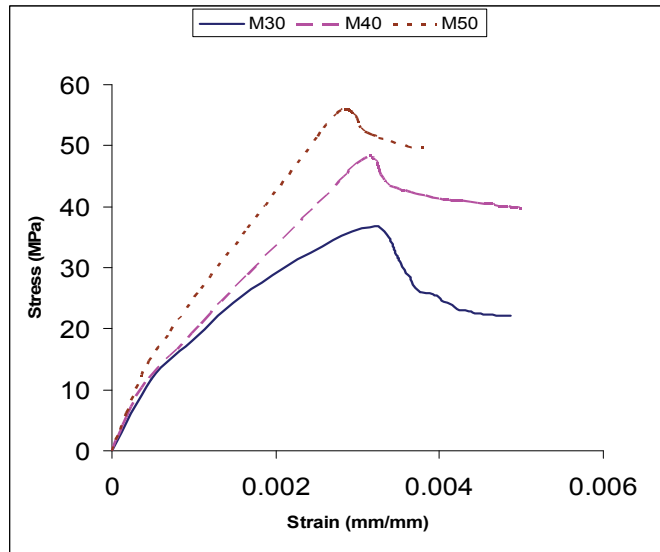

Figure 19: Stress-Strain Curves of M40 and M50 concrete

Now the M40 and M50 analytical models created with the help of established literature will be analyzed under one and two layers of confinement. The finite element model of the fabric cover remains the same as previously used and the thickness of each layer is also 1mm.

The following Figure 20 clearly demonstrates the effect of single layer confinement on M40 and M50 concrete.

The Table 12 compares the plain M40 and M50 models with single layer confined models of the same.

Table 12: Effect of single layer of confinement on M40 and M50 concrete

Grade of concrete	Unconfined Strength	Strength with one Layer of confinement	Increase over unconfined strength
M 40	48.4 MPa	56.4 MPa	16.5 %
M 50	56.1 MPa	63 MPa	12.3 %

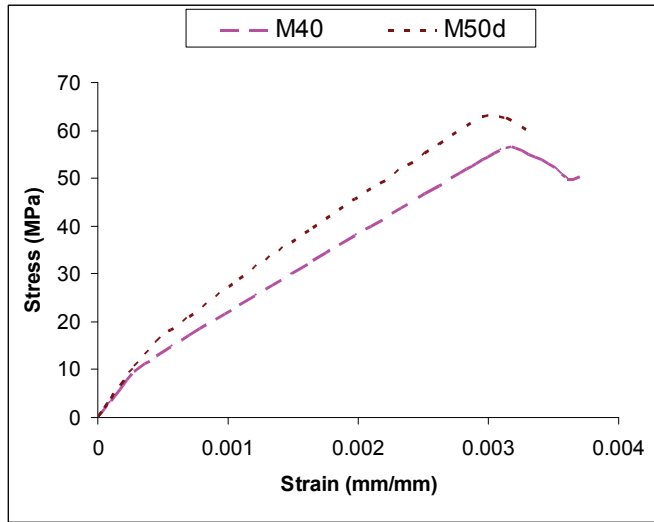From the Table 12 it can be inferred that the effect of single layer confinement has

Figure 20: Parametric models with one layer of confinement

been significant on the strength of the members. However, the effect decreased with increase in grade of the concrete member (12.3% increase for M50 compared to a 16.5% for M40), indicating that a particular confinement system can be used only for a particular range of concrete members and after that the effect of confinement diminishes.

Figure 21 shows the results of double layer confined models of M40 and M50 grade concrete.

Table 13 mentions the strength of M40 and M50 models with different layers of confinement.

Table 13: Effect of double layer confinement on M40 and M50 concrete

Grade	Plain Strength	1 Layer Strength	2 Layer Strength
M40	48.4 MPa	56.4 MPa	63.3 MPa
M50	56.1 MPa	63 MPa	69.2 MPa

Table 14 compares the increase in strength of the M40 and M50 models with each layer of confinement.
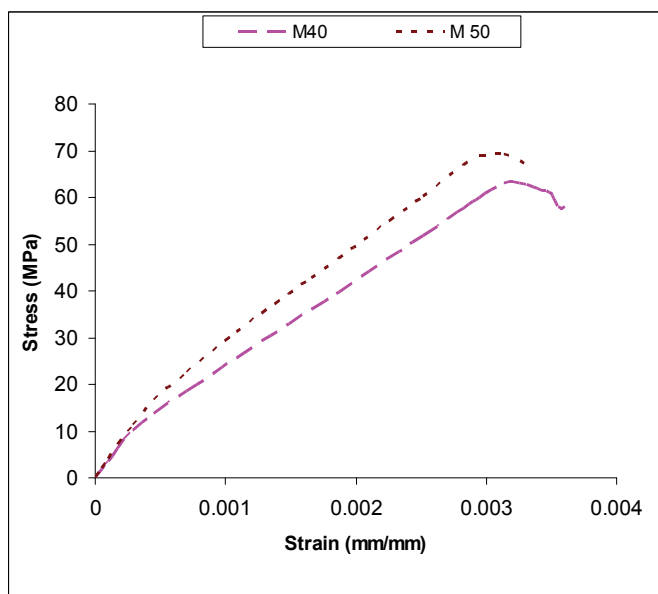
Figure 21: Parametric models with 2 layers of confinement

Table 14: Increase in strength w.r.t. layers of confinement

Grade	1 layer vs plain	2 layer vs plain	2 layer vs 1 layer
M40	16.5% increase	30.8% increase	12.2% increase
M50	12.3% increase	23.4% increase	9.8% increase

5   Summary and Conclusions

To study the effect of confinement on concrete members, experimental and analytical investigations have been carried out. Experimental investigations indicated that almost 35% increase in strength was obtained by means of single layered wrapping of the given fabric compared to plain concrete specimen and proved that confinement using E-Glass woven roving fabric results in considerable improvement over members load bearing capacity. Energy absorption is increased to 200% by means of double layer confinement and to 153% by means of single layer confinement of the given fabric. This effect is especially advantageous in case of seismic strengthening of structures. Further, the end failure was brittle mainly because of increased energy absorption and sudden release of energy. White patches indicating the debonding of fabric form concrete surfaces were observed before sudden failure and can be seen as warning signals before the collapse.

From the finite element analysis, it can be observed that the unconfined model (plain concrete) predicted the maximum strength of the member with an accuracy of 95%. The stress-strain response of the plain analytical model depicted the behavior of experimental plain concrete and hence the material model selected for concrete is correct. The response of single layer wrap on the plain analytical model was similar to experimental behavior and the analytical model was successful in predicting the maximum strength of the concrete member under single layer of confinement to an accuracy level of 90%. The double layered analytical model overestimated the maximum strength of the experimental model but this was because, the results obtained for double layer confinement during the experiment was lowered due to debonding of fabric layers. Hence the predictions of the double layer analytical model make sense. Also, the behavior of the stress-strain curve of the double layer wrapped analytical model was very similar to its experimental counterpart. Mesh sensitivity analysis was also performed in order to study the dependence of mesh element and mesh size on the behavior of the finite element models. Confinement of concrete members showed higher strength when the glass fabric was meshed with tetrahedral elements compared to hexagonal elements. From the parametric studies, it was observed that a particular confinement system depends on the strength of the member. Same confinement system will not be as effective on a higher strength concrete member as it will be in a lower strength concrete member. The effect of number of layers on strength diminished with increasing layers and hence the extent to which a structure can be strengthened by a certain strengthening system has a definite limit. The choice of a confinement system depends on the physical condition of the structure and the amount of strengthening required for a particular structure.

References

Ahmad, S. M.; Khaloo, A. R.; Irshaid, A. (1991): Behavior of concretespirally confined by fiberglass filaments. *Mag. Concrete Res.,* vol.43, no.156, pp.143–148.

Benzaid, R.; Chikh, N.E.; Mesbah, H. (2008): Behaviour of square column confined with GFRP composite wrap. *Journal of Civil Engineering and Management*, vol. 14, no.2, pp. 115–120.

De Laura L.; Tepfers, Ralejs. (2003): Comparitive Study of models on confinement of concrete cylinders with fiber reinforced polymer composites. *Journal of Composites for construction.*

Fam, A. Z.; Rizkalla, S. H. (2000): Concrete-filled FRP tubes for flexural and axial compression members. *Proc., ACMBS-3*, Ottawa, Canada, pp: 315–322.

Fardis, M. N.; Khalili, H. (1982): FRP-encased concrete as a structural material. *Mag. Concrete Res.,* vol.34, no.121, pp: 191–202.

Gu, H.; Zuo, Z. (2006): Compressive behaviors and failure modes of concrete cylinders reinforced by glass fabric. *Materials and Design,* vol.27, pp.601-104.

Harmon, T. G.; Slattery, K. T. (1992): Advanced composite confinement of concrete. 1st Int. *Conf. on Advanced Composite Materials in Bridges and Structures*, Sherbrooke, Que, Canada, pp: 299–306.

Saravanan, J.; Suguna, K.; Raghunath, P.N. (2010): Confined High Strength Concrete Columns: An Experimental Study. *American J. of Engineering and Applied Sciences*, vol.3 ,no.1,pp.133-137.

Kurt, C. E. (1978): Concrete filled structural plastic columns. *J. Struct. Div., ASCE*, vol.104, no.1, pp: 55–63.

Lam, L.; Teng, J. G. (2003): Stress-Strain Model for FRP-Confined Concrete for Design Application. 6th International Symposium on Fiber *Reinforced Polymer Reinforcement for Concrete Structures* (FRPRCS-6), K. H. Tan, ed., vol.2, pp. 601-612.

Shahawy, M.; Mirirman, A.; Beitelman, T. (2000): Tests and modeling of carbon wrapped concrete columns. *Journal of composites Part B: Engineering,* vol. 31, pp. 6-7.

Matthys, S.; Taerwe, L.; Audenaert, K. (1999): Tests on axially loaded concrete columns confined by fiber reinforced polymer sheet wrapping. *Proc., FRPRCS-4*, Baltimore, pp: 217–228.

Micelli, F.; Myers, J. J.; Murthy, S. (2001): Effect of environmental cycles on concrete cylinders confined with FRP. Proc., CCC2001 *Int. Conf. on Composites in Construction*, Porto, Portugal.

Miyauchi, K.; Nishibayashi, S.; Inoue, S. (1997): Estimation of strengthening effects with carbon fiber sheet for concrete column. Non-Metallic (FRP) *Reinforcement for Concrete Structures*, Proceedings of the Third International Symposium, vol.1, pp: 217–224.

Nanni, A., Bradford, N. M. (1995): FRP jacketed concrete under uniaxial compression. *Constr. Build. Mater.,* vol. 9, no.2, pp: 115–124.

Sangeetha, P. (2007): Analysis of FRP wrapped concrete columns under uniaxial

compression. *Journal of Scientific And Industrial research*, vol. 66, pp.235-242.

Picher, F.; Rochette, P.; Labossie're, P. (1996): Confinement of concrete cylinders with CFRP. *Proc., ICCI'96, Tucson*, Ariz., pp: 829–841.

Rochette, P.; Labossie're, P. (2000). Axial testing of rectangular column models confined with composites. *J. Compos. Constr.,* vol. 4, no.3, pp: 129–136.

Rousakis, T. (2001): Experimental investigation of concrete cylinders confined by carbon FRP sheets, under monotonic and cyclic axial compressive load. Research Rep., Chalmers *Univ. of Technology*, Go¨teborg, Sweden.

Saafi, M.; Toutanji, H. A.; Li, Z. (1999): Behavior of concrete columns confined with fiber reinforced polymer tubes. *ACI Mater. J.,* vol.96, no.4, pp: 500–509.

Saravanan, J.; Suguna, K.; Raghunath, P.N. (2010): Confined High Strength Concrete Columns: An Experimental Study. *American J. of Engineering and Applied Sciences,* vol.3, no.1, pp.133-137.

Toutanji, H. (1999): Stress-strain characteristics of concrete columns externally confined with advanced fiber composite sheets. *ACI Mater. J.,* vol.96, no.3, pp: 397–404.

Watanabe, K.; Nakamura, H.; Honda, Y.; Toyoshima, M.; Iso, M.; Fujimaki, T.; Kaneto, M.; Shirai, N. (1997). Confinement effect of FRP sheet on strength and ductility of concrete cylinders under uniaxial compression. *Proc., FRPRCS*-3, Sapporo, Japan, vol.1, pp: 233–240.

Wu, G.; Wu, Z. S.; Lu, Z. T. (2007): Design oriented stress-strain model for concrete prisms confined with FRP composites. *Construction and Building Materials*, vol.21, pp. 1107-1121.

Xiao, Y.; Wu, H. (2000): Compressive behavior of concrete confined by carbon fiber composite jackets. *J. Mater. Civ. Eng.*, vol.12, no.2, pp: 139–146.

Ye, L.; Zhang, S.; Mai, Y. W. (1998): Strengthening Efficiency of E-Glass Fibre Composite Jackets of Different Architectures for Concrete Columns. *Applied Composite Materials* , vol. 5, no.2, pp.109-122.